A study on the influence of inorganic ions, organic carbon, and microstructure on the hygroscopic property of soot

Zhanyu Su[1,2], Lanxiadi Chen[2,3], Yuan Liu[1,2], Peng Zhang[1], Tianzeng Chen[1], Biwu Chu[1,2], Mingjin Tang[2,3], Qingxin Ma[1,2*], Hong He[1,2]

[1]State Key Joint Laboratory of Environment Simulation and Pollution Control, Research Center for Eco-Environmental Sciences, Chinese Academy of Sciences, Beijing 100085, China

[2]College of Resources and Environment, University of Chinese Academy of Sciences, Beijing 100049, China

[3]State Key Laboratory of Organic Geochemistry, Guangzhou Institute of Geochemistry, Chinese Academy of Sciences, Guangdong 510640, China

Correspondence to: Qingxin Ma (qxma@rcees.ac.cn)

Abstract. Soot is a crucial component of aerosols in the atmosphere. Understanding the hygroscopicity of soot particles is important for studying their role as cloud condensation nuclei (CCN), as well as their chemical behavior and atmospheric lifetime. However, there is still a lack of comprehensive understanding regarding the factors that determine the hygroscopic properties of soot. In this work, the hygroscopic behavior of soot particles generated from different types of fuel combustion and aged with SO_2 for varying durations was measured by a vapor sorption analyser. Various characterizations of soot were conducted to understand the key factors that influence the hygroscopic properties of soot. It was found that water-soluble substances in soot facilitate the completion of monolayer water adsorption at low relative humidity and increase the number of water adsorption layers at high relative humidity. On the other hand, soot prepared from fuels burning typically lacks water-soluble inorganic ions and their hygroscopicity is primarily influenced by organic carbon (OC) and microstructure. Furthermore, the hygroscopicity of soot can be enhanced by the formation of sulfate due to heterogeneous oxidation of SO_2. These finding sheds light on the critical factors that affect soot hygroscopicity during water adsorption and allows for estimating the interaction between water molecules and soot particles in a humid atmosphere.

Keywords: soot, hygroscopicity, multilayer adsorption, water-soluble ions, organic carbon, microstructure, heterogeneous reaction

Introduction

Soot particles are produced by incomplete combustion processes of carbon-containing materials (Petzold et al., 2013). The current global emission of soot has been estimated to be 3-8 TgC per year (Forster et al., 2007). Soot aerosol can influence climate by directly absorbing solar radiation and affecting cloud formation and surface albedo through deposition on snow and ice (Liao et al., 2015; Peng et al., 2016), which results in the contribution of soot to anthropogenic radiative forcing second only to that of CO_2 (Bond et al., 2013; Cappa et al., 2012; Liu et al., 2017). In addition, soot particles can significantly enhance the atmospheric oxidation capacity (He et al., 2022) and contribute to the formation of secondary aerosols by providing active surface for the heterogeneous reactions of gaseous pollutants like NO_2, SO_2, and volatile organic compounds (VOCs) (Tritscher et al., 2011; Han et al., 2017; Zhang et al., 2022b; Liu et al., 2023). Moreover, soot particles also pose a health risk by causing and enhancing respiratory, cardiovascular, and allergic diseases (Janssen et al., 2011; Lin et al., 2011). Due to its significant effect on global climate change, regional air quality and human health, the physicochemical properties of soot have attracted much attention in recent decades.

Hygroscopicity is one of the most important physicochemical properties of soot, which largely determines the cloud condensation nuclei (CCN) activity as well as the consequent radiation forcing (Semeniuk et al., 2007; Ramanathan and Carmichael, 2008; Friedman et al., 2011). On the other hand, the hygroscopicity of atmospheric particles is important for their chemical behavior because water molecules were found to significantly affect the heterogeneous transformation of gaseous pollutants on soot surfaces (Zhao et al., 2017; He and He, 2020; Zhang et al., 2022b).

The hygroscopic behavior of soot has been widely studied. It was found that soot prepared in laboratory or commercial soot appears to be hydrophobic as there is no noticeable uptake of water at unsaturated humidity. For instance, the commercial soot and spark discharge soot particles shrunk with increasing RH during the growth factor measurements by hygroscopicity tandem differential mobility analysers (H-TDMA) (Weingartner et al., 1997; Henning et al., 2010). This was explained with a restructuring of the agglomerated particles. Due to the inverse Kelvin effect, water condenses in small angle cavities of soot particles, which leads to capillary forces on the branches of the aggregates and cause them to collapse. Different from the commercial soot and spark discharge soot, diesel soot, aircraft soot and biomass smoke particle showed obvious particle size growth with increasing RH (Popovicheva et al., 2008; Carrico et

al., 2010). This indicates that the chemical composition of soot is an important factor affecting its hygroscopicity. Our previous study suggested that combustion conditions could affect morphology and microstructure of soot, which has significant effect on the hygroscopicity (Han et al., 2012).

Soot aerosols experience internal mixing with other compounds (inorganic, organic, or inorganic/organic mixtures) as aging after their emission (Shiraiwa et al., 2007; Matsui et al., 2013). Field observations have demonstrated that the presence of BC-coating materials greatly influences both the hygroscopic properties and the CCN properties (or the wet removal) (Ohata et al., 2016; Li et al., 2018; Hu et al., 2021). Several laboratory studies have also simulated the hygroscopic changes of soot particles during atmospheric transport and aging. Soot particles generated from incomplete combustion of propane were exposed to the oxidation products of the OH-toluene reaction, resulting in an organic coating that increased the hygroscopicity of the particles (Qiu et al., 2012). Moreover, the aging process of propane flame soot through NO_2 oxidation of SO_2 was found to produce inorganic hydrophilic coating materials and significantly enhance the CCN activity of soot particles (Zhang et al., 2022a).

The hygroscopicity of soot can vary significantly depending on its source and aging processes, which has implications for regional air quality and climate. However, previous studies have often focused on specific factors influencing the hygroscopicity of a particular type of soot, lacking a comprehensive understanding of the key factors determining the hygroscopic properties of soot. In this study, we conducted measurements to determine the hygroscopicity of soot produced from different fuels and aged with SO_2 for different time. In addition, the chemical composition and microstructure of soot were characterized for each soot sample. The main objectives of this study were to compare the hygroscopicity of soot from different sources and analyze the effect of OC, water-soluble ions and microstructure on the multilayer adsorption of soot surface water. Moreover, the impact of heterogeneous aging reactions on the multilayer adsorption of water on the surface of soot particles was also explored. This study contributes to a deeper understanding of the hygroscopicity and atmospheric impacts of soot particles in the atmosphere.

2.Experimental section

2.1 Soot samples.

Prepared soot particles were obtained by burning n-hexane, decane or toluene (AR, Sinopharm Chemical Reagent Lo., Ltd) in a co-flow system as described in our previous studies (Han et al., 2012; Zhao et al., 2017). Briefly, the co-flow burner consisted of a diffusion flame maintained in a flow of synthetic air. Soot was collected on a quartz disc (7 cm in diameter) over diffusion flame and then stored in a brown bottle (Agilent). Diesel soot (DS) was collected from the diesel particle filter (DPF) of a China VI heavy-duty diesel engine (ISUZU from China). A diesel engine bench test was run under the conditions of World Harmonized Transient Cycle (WHTC). China VI fuels were used in the study, meeting the GB T32859-2016 standard. Printex U powder (U-soot) from Degussa (CAS No.: 1333-86-4) was used as a model soot. These types of soots are usually used in laboratory simulation as representative of soot in the atmosphere (Liu et al., 2010; Han et al., 2012; Zhang et al., 2022b).

The aging experiments were performed in a quartz flow tube reactor. Prior to the reaction, 0.05 g U-soot powder was placed into the quartz flow tube reactor. The experiments were maintained at 25 °C. Zero air was used as the carrier gas with a total flow rate about 700 ml min^{-1}. The SO_2 concentration was 5 ppm. The relative humidity (RH) of aging reaction was 50 % RH (recorded with Vaisala HMP110). To simulate solar irradiation, a high uniformity integrated xenon lamp (PLS-FX300HU, Beijing Perfectlight Technology Co., Ltd.) of 270 mW cm^{-2} was used as the light source. Its visible spectrum ranges from 330 to 850 nm.

2.2 Characterization of soot

A transmission electron microscope (H-7500, Hitachi) was used to investigate the morphologies of soot particles. DS sample was ultrasonically dispersed in ethanol while other soot samples were ultrasonically dispersed in ultrapure water (18.2 MΩ cm). Then, a droplet of suspension was deposited onto a Cu microgrid. An acceleration voltage of 200 kV was used for measurements. The diameter of particles was analyzed by ImageJ 1.41 software.

Raman spectra of soots were obtained with a Renishaw inVia Raman microscope system using a 532 nm excitation wavelength. The exposure time for each scan was 60 s. Data were acquired and analyzed using Renishaw WiRE 5.4 software.

The content of OC was measured using a thermal-optical transmittance OC/EC analyzer (Sunset laboratory Inc., Forest Grove, OR) with modified NIOSH 5040 protocol and produced four OC fractions (OC1, OC2, OC3, and OC4 at 150, 250, 450, and 550 °C respectively), OP (pyrolyzed organic) fraction (a pyrolyzed carbonaceous component determined when transmitted laser returned to its original intensity after the sample was exposed to oxygen), and three EC fractions (EC1, EC2, and EC3 at 550, 700, and 800 °C, respectively). OC is defined as OC1+OC2+OC3+OC4+OP and EC is defined as EC1+EC2+EC3-OP (Chow et al., 1993; Li et al., 2016).

The chemical compositions of OC in soots were identified via gas chromatography coupled with mass spectrometry (GC–MS, Agilent 6890–5973). 5 mg soot was first ultrasonically extracted for 10 min using 10 ml of dichloromethane (CH_2Cl_2), which was filtered through a quartz sand filter. The obtained supernatant liquid was subsequently concentrated using the N_2 blowing method for final analysis. The gas chromatograph was equipped with a DB-5MS 30 m × 0.25 mm × 0.25 mm capillary column and the mass spectrometer employed a quadrupole mass filter with a 70 eV electron impact ionizer. The temperature of the programmed temperature vaporizer was held at 270 °C. The initial oven temperature was set at 40 °C for 2 min, then increased step-by-step to 150 °C (by 5 °C min^{-1}) for 5 min, 280 °C (by 10 °C min^{-1}) for 10 min, and 320 °C (by 10 °C min^{-1}) for 5 min.

For ion chromatography (IC) measurement, about 5 mg of soot particles were extracted by ultrasonication with 10 mL ultrapure water (18.2 MΩ cm) for 10 min. Then, the extract was filtered through a 0.22 mm PTFE membrane filter. The obtained solution was analyzed using a Wayee IC-6200 ion chromatography system equipped with a SI-524E anionic analytical column. An eluent of 10 mM KOH was used at a flow rate of 1.0 mL min^{-1}.

2.3 Hygroscopic properties of soot

The hygroscopic properties of soots were investigated using a vapor sorption analyzer (VSA, Q5000 SA, TA Instruments), which has been applied to study hygroscopicity of atmospherically relevant particles in previous work (Chen et al., 2019; Gu et al., 2017). VSA utilizes a highly sensitive balance to measure the mass change of a sample as a function of RH at a given temperature. The instrument has a measurement range of 0−100 mg with a sensitivity of 0.01 μg, allowing for precise analysis. The temperature could be controlled in the range of 5−85 °C with an accuracy of 0.1 °C, and RH could be regulated in the range of 0−98 % with an absolute accuracy of 1 %. To ensure the accuracy of RH

measurements, we routinely measured deliquescence relative humidities (DRHs) of NaCl, $(NH_4)_2SO_4$, and KCl, and the difference between measured and theoretical DRHs did not exceed 1 %, confirming the reliability and accuracy of the instrument.

Hygroscopicity of soot was investigated at 25 °C. Figure 1 displays the change of RH and normalized sample mass with experimental time in a typical experiment. U-soot was dried at < 1 % RH and the sample mass under dry conditions was typically 1−5 mg. After that, RH increased step by step from 10 % to 90 %, with an increase of 20 % per step. At each point, the adsorption of water on samples was considered to reach an equilibrium when its mass change was < 0.05 % within 60 min.

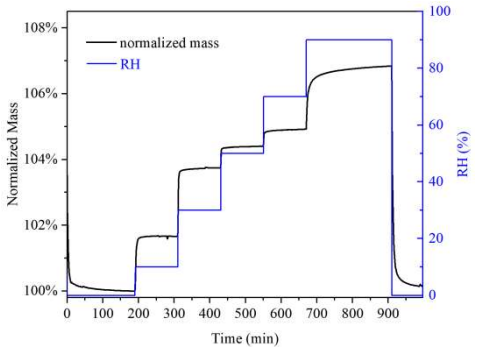

Figure 1. RH (blue curve, right y axis) and normalized sample mass (black curve, left y axis) as a function of experimental time during one experiment in which hygroscopic properties of U-soot were examined at 25 ºC.

3.Result and discussion

3.1The morphology and vapor adsorption isotherms of various soot

Figure 2 shows TEM images of soot samples. All soot samples exhibit a long chain like aggregate shape composed of typical spherical particles, which is consistent with previous studies (Han et al., 2012; Liu et al., 2010).

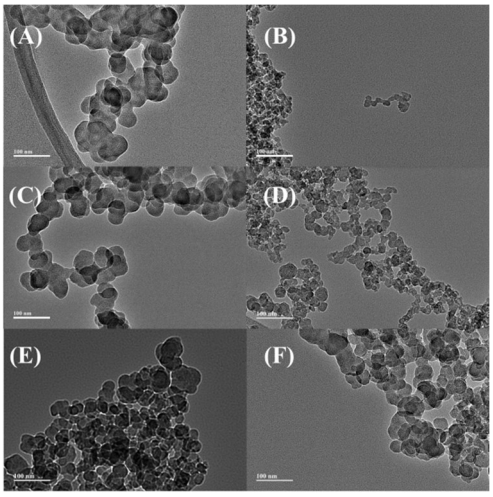

Figure 2. TEM images of n-hexane flame soot (A), decane flame soot (B), toluene flame soot (C), diesel soot (D), U-soot aggregates (E) before and (F) after aged with 5 ppm of SO_2 for 10 h.

Figure 3 shows the diameter distribution of soot particles. Particles exhibit a relatively uniform particle size distribution. Notably, the proportion of spherical particles with large diameter (> 35 nm) of aged U-soot was slightly greater than that of fresh U-soot. Nevertheless, the average particle diameter ($\bar{d}_p$) of U-soot and SO_2 aged U-soot are 39.55 nm and 41.60 nm, respectively, suggesting weak effect of SO_2 heterogeneous reaction on the size distribution of U-soot particles.

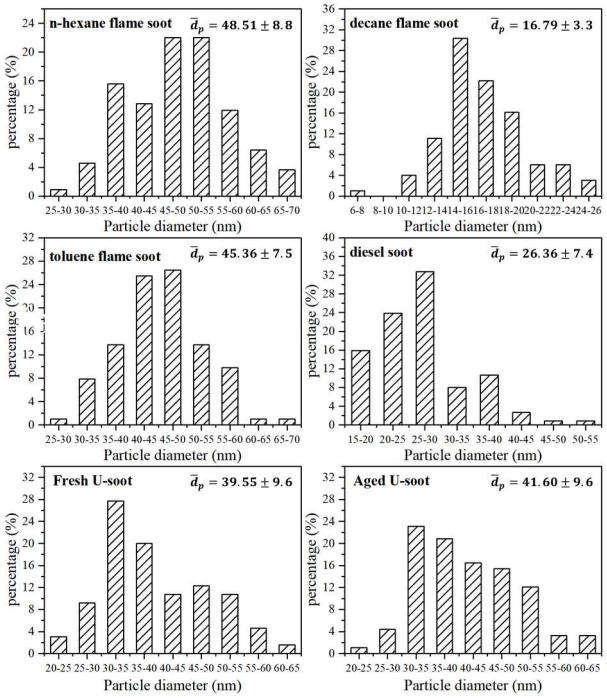

Figure 3. Diameter distribution of n-hexane flame soot, decane flame soot, toluene flame soot and diesel soot and U-soot particles before and after aged with 5 ppm of SO_2 for 10 h.

Figure 4 shows the normalized sample mass (normalized to that at < 1 % RH, m/m_0) as a function of RH for five types of soot. Three types of prepared soots (n-hexane flame soot, decane flame soot and toluene flame soot) exhibited lower water adsorption per unit mass sample under each RH condition compared to DS and U-soot particles. Specifically, at 90 % RH, DS showed the highest water adsorption among all soot samples, with a m/m_0 value of 1.138, followed by U-soot with a value of 1.067. Moreover, among the three prepared soots, decane flame soot exhibited the highest hygroscopicity with a normalized sample mass of 1.054 at 90 % RH.

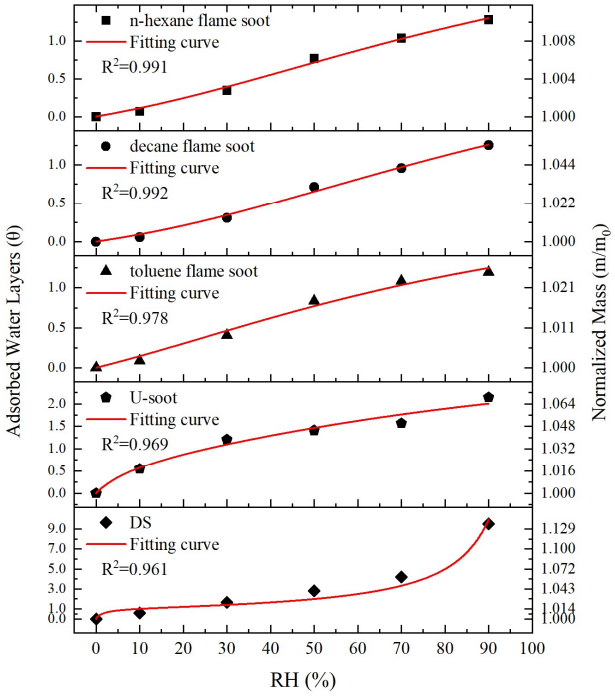

Figure 4. Water adsorption isotherms of soots, fitting curves (lines) with BET equation and the measured sample mass change (normalized to that at < 1 % RH, i.e., m/m$_0$) of soots as a function of RH (up to 90 % RH).

In order to further analyze the adsorption characteristics of water on soot, the isotherms of soot were fitted with the Brunauer-Emmett-Teller (BET) equation. As shown in Fig. 4, the isotherms of prepared soot and U-soot could be well fitted with three-parameters BET equation with the assumption of limited adsorbed water layers as following Eq. (1) (Brunauer et al., 1938; Goodman et al., 2001; Ma et al., 2010; Tang et al., 2016):

$$V = \frac{V_m c \frac{P}{P_0}}{1-\frac{P}{P_0}} \times \frac{1-(n+1)\left(\frac{P}{P_0}\right)^n + n\left(\frac{P}{P_0}\right)^{n+1}}{1+(c-1)\frac{P}{P_0} - c\left(\frac{P}{P_0}\right)^{n+1}} \quad (1)$$

Where, V is the volume of gas adsorbed at equilibrium pressure P, V_m is the volume of gas necessary to cover the surface of the adsorbent with a complete monolayer, P_0 is the saturation vapor pressure of the adsorbing gas at that temperature. n is an adjustable parameter given as the maximum number of layers of the adsorbing gas and is related to the pore size and properties of adsorbent. As a result, multilayer formation of adsorbing gas is limited to n layers at large values of P/P_0. The parameter c is the temperature-dependent constant related to the enthalpies of adsorption of the first and higher layers through Eq. (2) (Brunauer et al., 1938):

$$c = \exp\left(\frac{\Delta H_2^0 - \Delta H_1^0}{RT}\right) \quad (2)$$

Where, ΔH_1^0 is the standard enthalpy of adsorption of the first layer, and ΔH_2^0 is the standard enthalpy of adsorption on subsequent layers and is taken as the standard enthalpy of condensation, R is the gas constant, and T is the temperature in Kelvin.

For DS, a notable increase in sample mass was observed between 70 % and 90 % RH. This can be attributed to a significant rise in the number of adsorbed water layers within this specific RH range, which leads to the inability to describe the adsorption isotherm using the three-parameter BET equation. However, the two-parameter BET equation (Eq. (3)), assuming an unlimited number of adsorbed water layers, provides a better fit for the observed adsorption behavior of DS particles (Brunauer et al., 1938):

$$V = \frac{V_m c P}{(P_0 - P)\{1 + (c-1)(P/P_0)\}} \quad (3)$$

The fitted parameters, as shown in Table 1, provide valuable insights into the water adsorption behavior of different soot. The threshold relative humidity for one monolayer (MRH) for the fresh prepared soots is approximately 70 % RH. However, both U-soot and DS exhibit significantly lower MRH values (MRH_{DS} = 15 % RH, $MRH_{U\text{-}soot}$ = 25.5 % RH) compared to fresh prepared soot. This suggests that U-soot and DS have a higher affinity for water uptake at lower RH levels than fresh soot. At 90 % RH, prepared soot and U-soot particles were found to have approximately 1.2 and 2.1 layers of surface water adsorbed, respectively. Interestingly, DS showed around 9.5 layers adsorbed at 90 % RH, indicating a strong propensity for water adsorption.

The water-soluble ions like SO_4^{2-} and NO_3^- in soot samples were analyzed by IC, and the corresponding results are presented in Table 2. It was observed that the content of NO_3^- in all soot samples, except for DS, was approximately 0.2 μg mg^{-1}. However, DS exhibited a higher NO_3^- content of 1.44 μg mg^{-1}, which could be due to the aging of high concentration NOx coexisting in the exhaust pipe. Regarding SO_4^{2-}, the fresh prepared soots did not show any detectable levels of SO_4^{2-}. In contrast, both U-soot and DS displayed notable amounts of SO_4^{2-}, with U-soot having a content of 2.54 μg mg^{-1} and DS having the highest content of 11.46 μg mg^{-1}, respectively. These results indicate that water-soluble inorganic ions (e.g., nitrates and sulfates) are dominant factor for enhancing the hygroscopicity of soot, which is consistent with previous studies (Carrico et al., 2010; Popovicheva et al., 2010).

Table 1. Adsorption parameters for water uptake on soot.

Soot	BET area (m^2 g^{-1})	MRH (%)	*n*	*c*	R^2
n-hexane flame soot	26.27	68.0	2.84	1.01	0.991
toluene flame soot	70.97	67.2	2.47	1.37	0.978
decane flame soot	147.36	72.0	2.92	0.83	0.992
DS	47.93	15.0	---	66.95	0.961
U-soot	97.24	25.5	3.34	9.57	0.969
U-soot aged 2h	99.80	24.4	3.42	10.67	0.973
UBCU-soot aged 6h	101.46	25.0	3.59	9.82	0.956
U-soot aged 10h	98.96	26.2	3.82	8.58	0.944

Table 2. Mass concentration of SO_4^{2-} and NO_3^- and the ratio of OC/EC of soots.

Soot	Mass concentration of SO_4^{2-} (μg mg^{-1})	Mass concentration of NO_3^- (μg mg^{-1})	OC/EC
n-hexane flame soot	0.00	0.19	0.41±0.02
toluene flame soot	0.00	0.18	0.24±0.04
decane flame soot	0.00	0.22	0.16±0.06
DS	11.46	1.44	0.14±0.02
U-soot	2.55	0.24	0.12±0.03
U-soot aged 2h	4.83	0.20	---
U-soot aged 6h	7.14	0.19	---
U-soot aged 10h	9.61	0.20	---

3.2 The factors controlling the hygroscopic properties of prepared soot

Compared with DS and U-soot, prepared soots are more hydrophobic (Fig. 4) due to containing fewer water-soluble inorganic ions (Table 2). However, there are still significant differences in the hygroscopic behavior of soots prepared from different fuels. In order to analyze the differences in the hygroscopicity of different prepared soot, the relative content and species of OC and microstructure of soot were characterized. It was found that the n-hexane flame soot has the highest OC/EC ratio, followed by toluene

flame soot, and decane flame soot has the lowest OC/EC ratio (Table 2). It should be noted that the ratio of OC/EC is negatively correlated with their hygroscopicity, indicating that organic carbon is not conducive to the adsorption of water on the surface of soot. The impact of OC on the hygroscopicity of soot is still a subject of debate. Some field observations results have indicated that particles with high OC/EC ratio were preferentially removed by precipitation and the condensation of photochemically generated secondary organic carbon on soot particles could cause enhancement of hygroscopicity (Dasch and Cadle, 1989; Li et al., 2018). However, HTDMA measurements have shown that neither hygroscopicity nor droplet activation of the fresh propane soot particles depend on the OC content (Henning et al., 2012). Therefore, it is necessary to analyze the specific OC species present in prepared soot particles to gain a better understanding of their role in hygroscopicity.

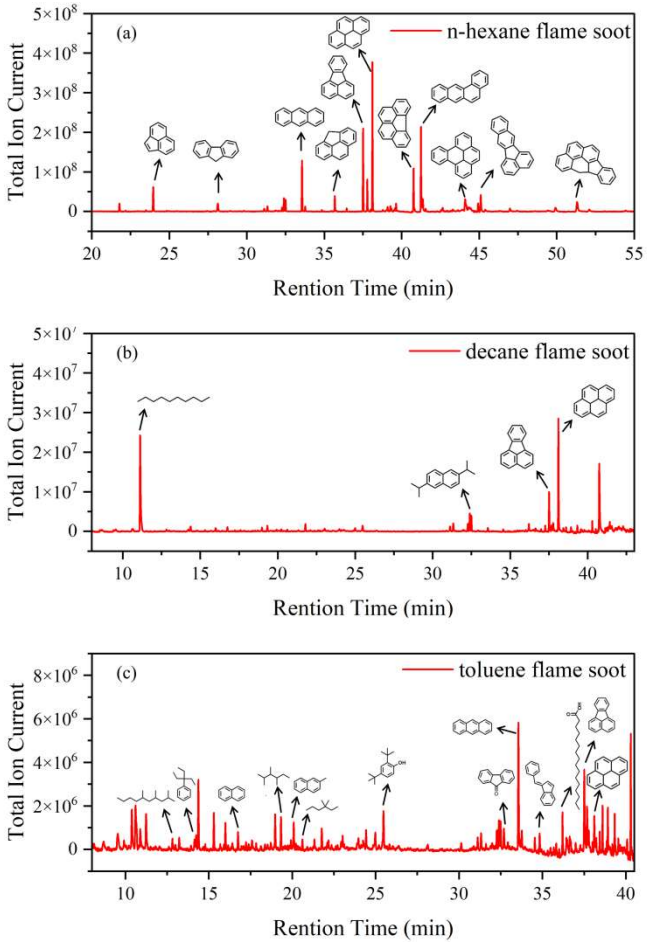

Figure 5. Total ion chromatogram extracts of prepared soots. (a) n-hexane flame soot. (b) decane flame soot. (c) toluene flame soot.

In order to obtain the composition of OC in different soot, the samples were extracted by CH_2Cl_2 and the extract was analyzed by GC-MS. Figure 5 shows the GC-MS analysis of OC extracted from different

prepared soot. The major components are polyaromatic hydrocarbons (PAHs) like Anthracene, Fluoranthene and Pyrene in all soot samples. It is well known that PAHs are usually formed simultaneously with soot during combustion. In n-hexane flame soot, PAHs are the main OC while other components are scarce, which is consistent with the results of Han et al (Han et al., 2012). For decane and toluene flame soot, long-chain alkanes such as decane or 2,3,4-trimethyl-hexane are present in the OC fraction. The characteristic features and peculiarities of the adsorption of water vapor on soot are primarily caused by the tendency of polar water molecules to form hydrogen bonds (Vartapetyan and Voloshchuk, 1995). However, PAHs are weakly polar organic compounds. Thus, the ability of π-electrons in the PAH aromatic ring to form weak hydrogen bonds with water molecules or the interactions with water molecules are either almost absent or are negligible (Lobunez, 1960). The oxygen-containing functional groups of organic compounds are substantial centers for the formation of hydrogen bonds with water molecules. In toluene flame soot, certain OC compounds (2,4-Di-tert-butylphenol, palmitic acid and 9-fluorenone) possess oxygen-containing functional groups like hydroxyl groups, carboxyl groups and quinone. However, these OC compounds also contain substantial hydrophobic parts (aromatic ring and hydrocarbon part). Despite a small amount, the contribution of these hydrophobic functional groups to the hygroscopicity could be dominant (Kireeva et al., 2010). For long-chain alkanes found in decane and toluene flame soot, they are typically considered hydrophobic. In general, OC constituents detected in these prepared soot samples could impede water adsorption on soot surfaces. Hence, the presence of these OC compounds leads to hydrophobic characteristics and diminishes the water adsorption capacity of prepared soot.

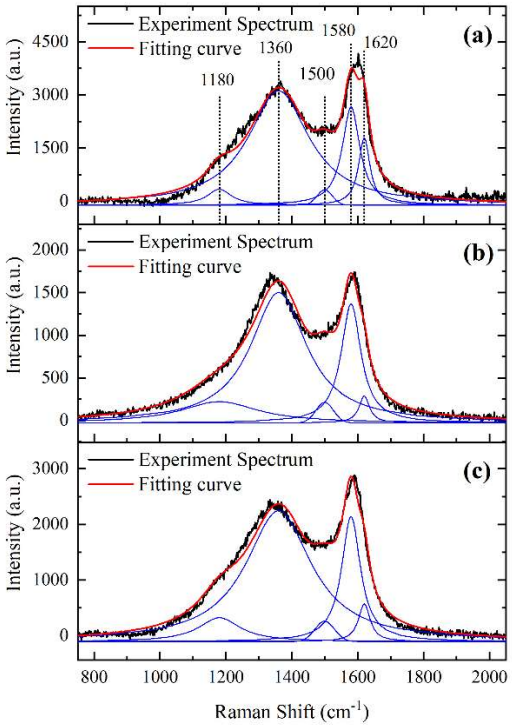

Figure 6. Raman spectra of (a) n-hexane, (b) decane and (c) toluene flame soot.

In order to study the relationship between the microstructure and vapor adsorption capacity of soot, Raman analysis on soot samples were conducted. Figure 6 shows the first-order Raman spectra of three prepared soots with good curve-fitting results ($R^2 > 0.982$), which display well known bands of soot near 1580 (G band) and 1360 cm^{-1} (D band). The G band is a typical characteristic of crystalline graphite, while the D band is only observed for disordered graphite. A detailed analysis of the first-order Raman spectra was performed using the five-band fitting procedure proposed by Sadezky (Sadezky et al., 2005). Four Lorentzian-shaped bands (D1, D2, D4, and G, centered at about 1360, 1620, 1180, and 1580 cm^{-1}, respectively) and one Gaussian-shaped band (D3, centered at around 1500 cm^{-1}) were used in the curve-fitting process (Sadezky et al., 2005; Ivleva et al., 2007; Liu et al., 2010). The D1 band arises from the A_{1g} symmetry mode of the disordered graphitic lattice located at the graphene layer edges. The D2 band is attributed to the E_{2g} symmetry stretching mode of the disordered graphitic lattice located at surface graphene layers. The D3 band originates from the amorphous carbon fraction of soot. The D4 band is related to the A_{1g} symmetry mode of the disordered graphitic lattice or C−C and C=C stretching vibrations of polyene-like structures, polyenes and ionic impurities also contribute to the D4 band (Sze et al., 2001; Sadezky et al., 2005). The G band is assigned to the ideal graphitic lattice with E_{2g} symmetry

vibration mode. The integral intensity ratio (I_D/I_G) of D and G bands was found to be related to the graphite crystallite size L_a (as determined by X-ray) (Knight and White, 1989; Schwan et al., 1996):

$$\frac{44}{L_a} = \left(\frac{I_D}{I_G}\right) \quad (4)$$

The intensities of D and G bands have been widely determined using the sum of D1 and D4 bands and the sum of D2 and G bands (Knauer et al., 2009). Table 3 shows similar changing trends between the I_{D4}/I_G of the three prepared soot samples and their hygroscopicity, while the L_a of the three prepared soot samples exhibits a negative correlation. These results imply that disordered graphitic lattice, polyenes, or ionic impurities (D4) could potentially serve as adsorption sites for water molecules. Moreover, graphite crystallite with smaller size could have higher adsorption capacity of water in soot.

Table 3. Parameters I_{D1}/I_G, I_{D4}/I_G, I_D/I_G and L_a of n-hexane, decane and toluene flame soot.

Fuels	I_{D1}/I_G	I_{D4}/I_G	I_D/I_G	L_a(Å)
n-hexane	2.59 ± 0.13	0.33 ± 0.01	2.87 ± 0.13	15.34 ± 0.69
toluene	2.87 ± 0.03	0.42 ± 0.09	3.23 ± 0.09	13.62 ± 0.38
decane	2.69 ± 0.08	0.75 ± 0.01	3.49 ± 0.15	12.63 ± 0.53

3.3 The effect of aging process on the hygroscopicity of soot.

Based on the hygroscopicity measurements of U-soot and DS (Fig. 4 and Table 2), it is evident that the coating water-soluble inorganic ions (e.g., sulfates and nitrates) can enhance the hygroscopicity of soot particles. Field observations have shown that the mass fractions of ammonium, sulfate, and nitrate increase with the aging of fresh biomass burning particles (Pratt et al., 2011). To investigate the impact of sulfate formation during the aging process on soot hygroscopicity, we aged U-soot with SO_2 for different durations and measured their hygroscopic properties accordingly. The results revealed an increase in sulfate ions on U-soot with longer aging times (Table 2) while the MRH of U-soot remains relatively unchanged with SO_2 aging (Table 1). However, at 90 % RH, the adsorbed water layers on U-soot increases with increasing aging times (Fig. 7). It should be noted that there is a good linear relationship ($R^2 = 0.9997$) between sulfate formed from SO_2 aging and adsorbed water mass at 90 % RH, where a corresponding water absorption mass increase by 1.82μg for every 1μg of SO_4^{2-} produced on the surface of U-soot.

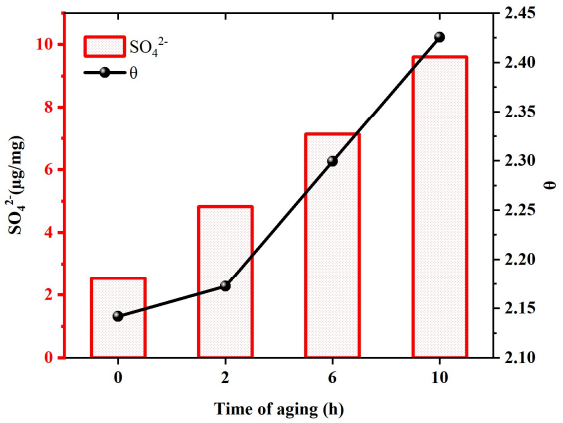

Figure 7. Amounts of sulfates on U-soot and the adsorbed water layers (θ) at 90 % RH of U-soot as a function of the time of aging.

Our previous study has found that the heterogeneous reaction between SO_2 and soot leads to the formation of sulfuric acid coating on soot (Zhang et al., 2022b). In this study, the sulfate detected on U-soot could also exist in the form of sulfuric acid. However, IC results demonstrated that the amount of newly generated sulfate on U-soot after 10 hours of aging was only 0.706 % of its original mass (Table 2). This small amount is insufficient to cause a significant difference in mass growth at low relative humidity such as cause little change in MRH. However, Kireeva et al. showed that the water adsorption isotherm of graphitized thermal soot coated with a small quantity of sulfuric acid showed a significant increase in the mass growth factor at relative humidity levels above 90 % (Kireeva et al., 2010). Zhang et al. found that coating with sulfuric acid could increase the mass growth factor of soot to above 1.2 at 80 % RH relative to fresh particles (Zhang et al., 2008). Our results also demonstrated that a noticeable augmentation in the amount of water adsorbed on SO_2 aged soot at 90 % RH, which is positively correlated with the amount of sulfate generated. Based on these findings, it can be concluded that varying amounts of sulfuric acid produced through heterogeneous oxidation on the surface of soot leads to noticeable differences in the amount of adsorbed water at high relative humidity. These findings are consistent with previous studies that coating with sulfuric acid can increase the hygroscopicity and ice nucleation activation of soot (Demott et al., 1999; Möhler et al., 2005; Wyslouzil et al., 1994).

4.Conclusion

In this study, we employed a vapor sorption analyzer to investigate the hygroscopicity of soot particles from different sources and at different stages of aging with sulfur dioxide. Multiple characterizations of

soot particles were also performed. DS and U-soot contained water-soluble ions, such as sulfates and nitrates, which enabled them to undergo monolayer adsorption at lower relative humidity and increase the number of water absorption layers at higher relative humidity. In contrast, fresh prepared soot particles, which have negligible amounts of water-soluble ions, were more hydrophobic. Their hygroscopicity mainly depended on the organic carbon content and microstructure. Lower content of hydrophobic OC and more disordered graphitic lattice, polyenes, or ionic impurities made prepared soot particles more prone to water adsorption. The aging of U-soot particles with SO_2 resulted in the formation of water-soluble sulfate ions, which promotes an increase in the hygroscopicity of soot particles. This study analyzed the key factors determining the hygroscopic property of soot, which can improve our understanding of the hygroscopic behavior of fresh soot and help to evaluate changes in hygroscopicity during the heterogeneous reactions of soot particles with pollutant gases in future studies.

Data availability

The experimental data are available upon request to the first or corresponding authors

Author Contributions

QM contributed to the conception of the study, ZS and LC designed and conducted this experiment, YL helped to prepare samples. QM, PZ, TC, BC, MT and HH helped perform the analysis with constructive discussions. ZS and QM wrote the paper with input from all coauthors. All authors contributed to the final paper.

Competing interests

The authors declare that they have no conflict of interest.

Acknowledge

This work was supported by the National Key R&D Program of China (2022YFC3701004), and the National Natural Science Foundation of China (No. 22188102), The authors also appreciate the Youth Innovation Promotion Association, CAS (Y2022021).

Reference

Bond, T. C., Doherty, S. J., Fahey, D. W., Forster, P. M., Berntsen, T., DeAngelo, B. J., Flanner, M. G., Ghan, S., Kaercher, B., Koch, D., Kinne, S., Kondo, Y., Quinn, P. K., Sarofim, M. C., Schultz, M. G., Schulz, M., Venkataraman, C., Zhang, H., Zhang, S., Bellouin, N., Guttikunda, S. K., Hopke, P. K., Jacobson, M. Z., Kaiser, J. W., Klimont, Z., Lohmann, U., Schwarz, J. P., Shindell, D., Storelvmo, T., Warren, S. G., and Zender, C. S.: Bounding the role of black carbon in the climate system: A scientific assessment, Journal of Geophysical Research-Atmospheres, 118, 5380-5552, 10.1002/jgrd.50171, 2013.

Brunauer, S., Emmett, P. H., and Teller, E.: Adsorption of gases in multimolecular layers, Journal of the American Chemical Society, 60, 309-319, 10.1021/ja01269a023, 1938.

Cappa, C. D., Onasch, T. B., Massoli, P., Worsnop, D. R., Bates, T. S., Cross, E. S., Davidovits, P., Hakala, J., Hayden, K. L., Jobson, B. T., Kolesar, K. R., Lack, D. A., Lerner, B. M., Li, S.-M., Mellon, D., Nuaaman, I., Olfert, J. S., Petaja, T., Quinn, P. K., Song, C., Subramanian, R., Williams, E. J., and Zaveri, R. A.: Radiative Absorption Enhancements Due to the Mixing State of Atmospheric Black Carbon, Science, 337, 1078-1081, 10.1126/science.1223447, 2012.

Carrico, C. M., Petters, M. D., Kreidenweis, S. M., Sullivan, A. P., McMeeking, G. R., Levin, E. J. T., Engling, G., Malm, W. C., and Collett, J. L., Jr.: Water uptake and chemical composition of fresh aerosols generated in open burning of biomass, Atmospheric Chemistry and Physics, 10, 5165-5178, 10.5194/acp-10-5165-2010, 2010.

Chen, L., Chen, Y., Chen, L., Gu, W., Peng, C., Luo, S., Song, W., Wang, Z., and Tang, M.: Hygroscopic Properties of 11 Pollen Species in China, Acs Earth and Space Chemistry, 3, 2678-2683, 10.1021/acsearthspacechem.9b00268, 2019.

Chow, J. C., Watson, J. G., Pritchett, L. C., Pierson, W. R., Frazier, C. A., and Purcell, R. G.: THE DRI THERMAL OPTICAL REFLECTANCE CARBON ANALYSIS SYSTEM - DESCRIPTION, EVALUATION AND APPLICATIONS IN UNITED-STATES AIR-QUALITY STUDIES, Atmospheric Environment Part a-General Topics, 27, 1185-1201, 10.1016/0960-1686(93)90245-t, 1993.

Dasch, J. M. and Cadle, S. H.: Atmospheric Carbon Particles in the Detroit Urban Area: Wintertime Sources and Sinks, Aerosol Science and Technology, 10, 236-248, 10.1080/02786828908600508, 1989.

DeMott, P. J., Chen, Y., Kreidenweis, S. M., Rogers, D. C., and Sherman, D. E.: Ice formation by black carbon particles, Geophysical Research Letters, 26, 2429-2432, 10.1029/1999gl900580, 1999.

Forster, P., Ramaswamy, V., Artaxo, P., Berntsen, T., Betts, R., Fahey, D. W., Haywood, J., Lean, J., Lowe, D. C., Myhre, G., Nganga, J., Prinn, R., Raga, G., Schulz, M., and Van Dorland, R.: Changes in Atmospheric Constituents and in Radiative Forcing, Ar4 Climate Change 2007: The Physical Science Basis: Contribution of Working Group I to the Fourth Assessment Report of the Intergovernmental Panel on Climate Change, 129-234 pp.2007.

Friedman, B., Kulkarni, G., Beranek, J., Zelenyuk, A., Thornton, J. A., and Cziczo, D. J.: Ice nucleation and droplet formation by bare and coated soot particles, Journal of Geophysical Research-Atmospheres, 116, D17203, 10.1029/2011jd015999, 2011.

Goodman, A. L., Bernard, E. T., and Grassian, V. H.: Spectroscopic study of nitric acid and water adsorption on oxide particles: Enhanced nitric acid uptake kinetics in the presence of adsorbed water, Journal of Physical Chemistry A, 105, 6443-6457, 10.1021/jp0037221, 2001.

Gu, W., Li, Y., Zhu, J., Jia, X., Lin, Q., Zhang, G., Ding, X., Song, W., Bi, X., Wang, X., and Tang, M.: Investigation of water adsorption and hygroscopicity of atmospherically relevant particles using a commercial vapor sorption analyzer, Atmospheric Measurement Techniques, 10, 3821-3832, 10.5194/amt-10-3821-2017, 2017.

Han, C., Liu, Y., and He, H.: Heterogeneous reaction of NO(2) with soot at different relative humidity, Environ Sci Pollut Res Int, 24, 21248-21255, 10.1007/s11356-017-9766-y, 2017.

Han, C., Liu, Y., Liu, C., Ma, J., and He, H.: Influence of combustion conditions on hydrophilic properties and microstructure of flame soot, J Phys Chem A, 116, 4129-4136, 10.1021/jp301041w, 2012.

He, G., Ma, J., Chu, B., Hu, R., Li, H., Gao, M., Liu, Y., Wang, Y., Ma, Q., Xie, P., Zhang, G., Zeng, X. C., Francisco, J. S., and He, H.: Generation and Release of OH Radicals from the Reaction of H(2) O with O(2) over Soot, Angew Chem Int Ed Engl, 61, e202201638, 10.1002/anie.202201638, 2022.

He, G. Z. and He, H.: Water Promotes the Oxidation of SO2 by O-2 over Carbonaceous Aerosols, Environmental Science & Technology, 54, 7070-7077, 10.1021/acs.est.0c00021, 2020.

Henning, S., Ziese, M., Kiselev, A., Saathoff, H., Moehler, O., Mentel, T. F., Buchholz, A., Spindler, C., Michaud, V., Monier, M., Sellegri, K., and Stratmann, F.: Hygroscopic growth and droplet activation of soot particles: uncoated, succinic or sulfuric acid coated, Atmospheric Chemistry and Physics, 12, 4525-4537, 10.5194/acp-12-4525-2012, 2012.

Henning, S., Wex, H., Hennig, T., Kiselev, A., Snider, J. R., Rose, D., Dusek, U., Frank, G. P., Pöschl, U., Kristensson, A., Bilde, M., Tillmann, R., Kiendler-Scharr, A., Mentel, T. F., Walter, S., Schneider,

J., Wennrich, C., and Stratmann, F.: Soluble mass, hygroscopic growth, and droplet activation of coated soot particles during LACIS Experiment in November (LExNo), Journal of Geophysical Research-Atmospheres, 115, D11206, 10.1029/2009jd012626, 2010.

Hu, D., Wang, Y., Yu, C., Xie, Q., Yue, S., Shang, D., Fang, X., Joshi, R., Liu, D., Allan, J., Wu, Z., Hu, M., Fu, P., and McFiggans, G.: Vertical profile of particle hygroscopicity and CCN effectiveness during winter in Beijing: insight into the hygroscopicity transition threshold of black carbon, Faraday Discuss, 226, 239-254, 10.1039/d0fd00077a, 2021.

Ivleva, N. P., Messerer, A., Yang, X., Niessner, R., and Poeschl, U.: Raman microspectroscopic analysis of changes in the chemical structure and reactivity of soot in a diesel exhaust aftertreatment model system, Environmental Science & Technology, 41, 3702-3707, 10.1021/es0612448, 2007.

Janssen, N. A. H., Hoek, G., Simic-Lawson, M., Fischer, P., van Bree, L., ten Brink, H., Keuken, M., Atkinson, R. W., Anderson, H. R., Brunekreef, B., and Cassee, F. R.: Black Carbon as an Additional Indicator of the Adverse Health Effects of Airborne Particles Compared with PM10 and PM2.5, Environmental Health Perspectives, 119, 1691-1699, 10.1289/ehp.1003369, 2011.

Kireeva, E. D., Popovicheva, O. B., Khokhlova, T. D., and Shoniya, N. K.: Laboratory simulation of the interaction of water molecules with carbonaceous aerosols in the atmosphere, Moscow University Physics Bulletin, 65, 510-515, 10.3103/s0027134910060159, 2010.

Knauer, M., Schuster, M. E., Su, D. S., Schlögl, R., Niessner, R., and Ivleva, N. P.: Soot Structure and Reactivity Analysis by Raman Microspectroscopy, Temperature-Programmed Oxidation, and High-Resolution Transmission Electron Microscopy, Journal of Physical Chemistry A, 113, 13871-13880, 10.1021/jp905639d, 2009.

Knight, D. S. and White, W. B.: Characterization of diamond films by Raman spectroscopy, Journal of Materials Research, 4, 385-393, 10.1557/JMR.1989.0385, 1989.

Li, C., Hu, Y., Chen, J., Ma, Z., Ye, X., Yang, X., Wang, L., Wang, X., and Mellouki, A.: Physiochemical properties of carbonaceous aerosol from agricultural residue burning: Density, volatility, and hygroscopicity, Atmospheric Environment, 140, 94-105, 10.1016/j.atmosenv.2016.05.052, 2016.

Li, K., Ye, X., Pang, H., Lu, X., Chen, H., Wang, X., Yang, X., Chen, J., and Chen, Y.: Temporal variations in the hygroscopicity and mixing state of black carbon aerosols in a polluted megacity area, Atmospheric Chemistry and Physics, 18, 15201-15218, 10.5194/acp-18-15201-2018, 2018.

Liao, H., Chang, W., and Yang, Y.: Climatic Effects of Air Pollutants over China: A Review, Advances in Atmospheric Sciences, 32, 115-139, 10.1007/s00376-014-0013-x, 2015.

Lin, W., Huang, W., Zhu, T., Hu, M., Brunekreef, B., Zhang, Y., Liu, X., Cheng, H., Gehring, U., Li, C., and Tang, X.: Acute Respiratory Inflammation in Children and Black Carbon in Ambient Air before and during the 2008 Beijing Olympics, Environmental Health Perspectives, 119, 1507-1512, 10.1289/ehp.1103461, 2011.

Liu, D., Whitehead, J., Alfarra, M. R., Reyes-Villegas, E., Spracklen, D. V., Reddington, C. L., Kong, S., Williams, P. I., Ting, Y.-C., Haslett, S., Taylor, J. W., Flynn, M. J., Morgan, W. T., McFiggans, G., Coe, H., and Allan, J. D.: Black-carbon absorption enhancement in the atmosphere determined by particle mixing state, Nature Geoscience, 10, 184-U132, 10.1038/ngeo2901, 2017.

Liu, Y., He, G., Chu, B., Ma, Q., and He, H.: Atmospheric heterogeneous reactions on soot: A review, Fundamental Research, 3, 579-591, https://doi.org/10.1016/j.fmre.2022.02.012, 2023.

Liu, Y., Liu, C., Ma, J., Ma, Q., and He, H.: Structural and hygroscopic changes of soot during heterogeneous reaction with O-3, Physical Chemistry Chemical Physics, 12, 10896-10903, 10.1039/c0cp00402b, 2010.

Lobunez, W.: Book Reviews : The Hydrogen Bond. , Textile Research Journal, 30, 1006-1007, 10.1177/004051756003001217, 1960.

Ma, Q., He, H., and Liu, Y.: In situ DRIFTS study of hygroscopic behavior of mineral aerosol, Journal of Environmental Sciences, 22, 555-560, 10.1016/s1001-0742(09)60145-5, 2010.

Matsui, H., Koike, M., Kondo, Y., Moteki, N., Fast, J. D., and Zaveri, R. A.: Development and validation of a black carbon mixing state resolved three-dimensional model: Aging processes and radiative impact, Journal of Geophysical Research: Atmospheres, 118, 2304-2326, 10.1029/2012jd018446, 2013.

Möhler, O., Büttner, S., Linke, C., Schnaiter, M., Saathoff, H., Stetzer, O., Wagner, R., Krämer, M., Mangold, A., Ebert, V., and Schurath, U.: Effect of sulfuric acid coating on heterogeneous ice nucleation by soot aerosol particles, Journal of Geophysical Research, 110, D11210, 10.1029/2004jd005169, 2005.

Ohata, S., Schwarz, J. P., Moteki, N., Koike, M., Takami, A., and Kondo, Y.: Hygroscopicity of materials internally mixed with black carbon measured in Tokyo, Journal of Geophysical Research: Atmospheres, 121, 362-381, 10.1002/2015jd024153, 2016.

Peng, J., Hu, M., Guo, S., Du, Z., Zheng, J., Shang, D., Zamora, M. L., Zeng, L., Shao, M., Wu, Y.-S., Zheng, J., Wang, Y., Glen, C. R., Collins, D. R., Molina, M. J., and Zhang, R.: Markedly enhanced

absorption and direct radiative forcing of black carbon under polluted urban environments, Proceedings of the National Academy of Sciences of the United States of America, 113, 4266-4271, 10.1073/pnas.1602310113, 2016.

Petzold, A., Ogren, J. A., Fiebig, M., Laj, P., Li, S. M., Baltensperger, U., Holzer-Popp, T., Kinne, S., Pappalardo, G., Sugimoto, N., Wehrli, C., Wiedensohler, A., and Zhang, X. Y.: Recommendations for reporting "black carbon" measurements, Atmospheric Chemistry and Physics, 13, 8365-8379, 10.5194/acp-13-8365-2013, 2013.

Popovicheva, O., Persiantseva, N. M., Shonija, N. K., DeMott, P., Koehler, K., Petters, M., Kreidenweis, S., Tishkova, V., Demirdjian, B., and Suzanne, J.: Water interaction with hydrophobic and hydrophilic soot particles, Physical Chemistry Chemical Physics, 10, 2332-2344, 10.1039/b718944n, 2008.

Popovicheva, O. B., Kireeva, E. D., Timofeev, M. A., Shonija, N. K., and Mogil'nikov, V. P.: Carbonaceous aerosols of aviation and shipping emissions, Izvestiya Atmospheric and Oceanic Physics, 46, 339-346, 10.1134/s0001433810030072, 2010.

Pratt, K. A., Murphy, S. M., Subramanian, R., DeMott, P. J., Kok, G. L., Campos, T., Rogers, D. C., Prenni, A. J., Heymsfield, A. J., Seinfeld, J. H., and Prather, K. A.: Flight-based chemical characterization of biomass burning aerosols within two prescribed burn smoke plumes, Atmospheric Chemistry and Physics, 11, 12549-12565, 10.5194/acp-11-12549-2011, 2011.

Qiu, C., Khalizov, A. F., and Zhang, R.: Soot Aging from OH-Initiated Oxidation of Toluene, Environmental Science & Technology, 46, 9464-9472, 10.1021/es301883y, 2012.

Ramanathan, V. and Carmichael, G.: Global and regional climate changes due to black carbon, Nature Geoscience, 1, 221-227, 10.1038/ngeo156, 2008.

Sadezky, A., Muckenhuber, H., Grothe, H., Niessner, R., and Poschl, U.: Raman micro spectroscopy of soot and related carbonaceous materials: Spectral analysis and structural information, Carbon, 43, 1731-1742, 10.1016/j.carbon.2005.02.018, 2005.

Schwan, J., Ulrich, S., Batori, V., Ehrhardt, H., and Silva, S. R. P.: Raman spectroscopy on amorphous carbon films, Journal of Applied Physics, 80, 440-447, 10.1063/1.362745, 1996.

Semeniuk, T. A., Wise, M. E., Martin, S. T., Russell, L. M., and Buseck, P. R.: Hygroscopic behavior of aerosol particles from biomass fires using environmental transmission electron microscopy, Journal of Atmospheric Chemistry, 56, 259-273, 10.1007/s10874-006-9055-5, 2007.

Shiraiwa, M., Kondo, Y., Moteki, N., Takegawa, N., Miyazaki, Y., and Blake, D. R.: Evolution of mixing state of black carbon in polluted air from Tokyo, Geophysical Research Letters, 34, L16803, 10.1029/2007gl029819, 2007.

Sze, S. K., Siddique, N., Sloan, J. J., and Escribano, R.: Raman spectroscopic characterization of carbonaceous aerosols, Atmospheric Environment, 35, 561-568, 10.1016/s1352-2310(00)00325-3, 2001.

Tang, M., Cziczo, D. J., and Grassian, V. H.: Interactions of Water with Mineral Dust Aerosol: Water Adsorption, Hygroscopicity, Cloud Condensation, and Ice Nucleation, Chemical Reviews, 116, 4205-4259, 10.1021/acs.chemrev.5b00529, 2016.

Tritscher, T., Juranyi, Z., Martin, M., Chirico, R., Gysel, M., Heringa, M. F., DeCarlo, P. F., Sierau, B., Prevot, A. S. H., Weingartner, E., and Baltensperger, U.: Changes of hygroscopicity and morphology during ageing of diesel soot, Environmental Research Letters, 6, 034026, 10.1088/1748-9326/6/3/034026, 2011.

Vartapetyan, R. S. and Voloshchuk, A. M.: Adsorption mechanism of water molecules on carbon adsorbents, Uspekhi Khimii, 64, 1055-1072, 1995.

Weingartner, E., Burtscher, H., and Baltensperger, U.: Hygroscopic properties of carbon and diesel soot particles, Atmospheric Environment, 31, 2311-2327, 10.1016/s1352-2310(97)00023-x, 1997.

Wyslouzil, B. E., Carleton, K. L., Sonnenfroh, D. M., Rawlins, W. T., and Arnold, S.: OBSERVATION OF HYDRATION OF SINGLE, MODIFIED CARBON AEROSOLS, Geophysical Research Letters, 21, 2107-2110, 10.1029/94gl01588, 1994.

Zhang, F., Peng, J., Chen, L., Collins, D., Li, Y., Jiang, S., Liu, J., and Zhang, R.: The effect of black carbon aging from NO2 oxidation of SO2 on its morphology, optical and hygroscopic properties, Environmental Research, 212, 113238, 10.1016/j.envres.2022.113238, 2022a.

Zhang, P., Chen, T., Ma, Q., Chu, B., Wang, Y., Mu, Y., Yu, Y., and He, H.: Diesel soot photooxidation enhances the heterogeneous formation of H(2)SO(4), Nat Commun, 13, 5364, 10.1038/s41467-022-33120-3, 2022b.

Zhang, R., Khalizov, A. F., Pagels, J., Zhang, D., Xue, H., and McMurry, P. H.: Variability in morphology, hygroscopicity, and optical properties of soot aerosols during atmospheric processing, Proceedings of the National Academy of Sciences of the United States of America, 105, 10291-10296, 10.1073/pnas.0804860105, 2008.

530 Zhao, Y., Liu, Y., Ma, J., Ma, Q., and He, H.: Heterogeneous reaction of SO2 with soot: The roles of relative humidity and surface composition of soot in surface sulfate formation, Atmospheric Environment, 152, 465-476, 10.1016/j.atmosenv.2017.01.005, 2017.